

Research Paper

Supercontinuum Generation in Silica Plasmonic Waveguide by Bright Soliton

Maryam Dehghani¹, Mohsen Hatami^{*2}, Abdolrasoul Gharaati¹

¹ Physics Department, Payame Noor University, Tehran, Iran.

² Faculty of Physics, Shiraz University of Technology, Shiraz, Iran.

Received: 24 Sep. 2021

Revised: 12 Oct. 2021

Accepted: 16 Nov. 2021

Published: 15 Dec. 2021

Use your device to scan
and read the article
online



Keywords:

Nonlinear Plasmonic Waveguide, Supercontinuum Generation, Nonlinear Raman Scattering, Self-Steepening

Abstract

We study the supercontinuum generation in a nonlinear silica single layer plasmonic waveguide. A major part of spectral broadening is related to soliton dynamics when an ultra-short pulse is launched in waveguide with anomalous GVD. Production of supercontinuum with 10th, 15th and 30th, orders bright solitons by considering all the nonlinear effects and dispersions i.e., inter-pulse Raman scattering, self-steepening, self-phase modulation, cross phase modulation, which indicates the existence of a supercontinuum propagation about 20 times broadening than initial width of input spectrum.

Also, we consider the absorption effect of plasmonic waveguide by calculating propagation length from propagation constant. The propagation length of plasmonic is compared with the waveguide length and nonlinear length. At wavelength $1.22\mu\text{m}$, the propagation length is obtained in the order of waveguide length which means one can consider the effect of absorption cannot alter the results. The nonlinear plasmonic waveguides are suitable for integrated photonics because of subwavelength confinement of plasmonic waveguides.

Citation: Dehghani Maryam, Hatami Mohsen, Gharaati Abdolrasoul. Supercontinuum Generation in Silica Plasmonic Waveguide by Bright Soliton.

Journal of Optoelectrical Nanostructures. 2021; 6 (4): 109-136

DOI: [10.30495/IOPN.2022.28937.1236](https://doi.org/10.30495/IOPN.2022.28937.1236)

***Corresponding author:** Hatami Mohsen

Address: Faculty of Physics, Shiraz University of Technology, Shiraz, Iran.

Tell: 00989131518991.

Email: hatami@sutech.ac.ir

1. Introduction

Spectral broadening and the generation of new frequency components are the intrinsic features of nonlinear optics. Because of these novel characteristics of nonlinear optics, it is possible to produce an artificial white light with unique spectral properties having high brightness. Under such a process, an ultra-short optical pulse propagates through a nonlinear medium experiencing extreme spectral broadening. Owing to its broad and continuous spectrum, such extreme spectral broadening is generally called supercontinuum (SC) [3,4].

The generation of white laser in terms of SC is an important phenomenon having great physical implications. It certainly offers novel solutions in the field of optical communication, coherent tomography, multiplex light sources for nonlinear spectroscopy, biomedical lasers, etc. [5]. The mechanism of SC generation is dominated by soliton dynamics when a femtosecond pulse is used as a pump. Higher-order dispersions (HODs) play a significant role in modulating and controlling the spectrum.

SPM can produce considerable spectral broadening at the fiber output. Another nonlinear mechanism that can generate new wavelengths is SRS. Even if the peak power is not large enough to reach the Raman threshold, SRS can amplify the pulse spectrum on the long-wavelength side.

FWM is a nonlinear process that can create sidebands on both sides of the pulse spectrum, provided a phase-matching condition is satisfied, and it is often behind a supercontinuum generated using optical fibers. FWM is also a reason for dispersive properties of the fiber play a critical role in the formation of a supercontinuum.

Fission of an N th-order soliton produces N fundamental solitons. All these solitons are shorter than the original input pulse, the shortest one being narrower by a factor of $(2N-1)$. The short pulses are affected by intrapulse Raman scattering and their spectra shift rapidly toward longer and longer wavelengths with further propagation inside the fiber.

Nonlinear microstructural fibers, including crystal photonic fiber, are a good environment for SC production, here, we first use nano plasmonic waveguides to investigate supercontinuum generation.

Due to its distinctive features, plasmonic has been heavily taken into account in recent years, especially because of its ability to enclose light in very small volumes [6-7], Plasmonic is based on the process of interaction between electromagnetic waves and conduction electrons in metals, Plasmonic can be used for applications in nonlinear optics which, due to the high field intensity in the plasmonic waveguides, the nonlinear effects in these waveguides are bigger

than that of dielectric fiber optics[8].

The goal of scientists working in the fields of nanoscience, plasmonic and metamaterials is to achieve complete control of the optical energy flowing at the nanoscale [9], this goal appears to be partly achieved by using nonlinear plasmonic waveguides in which the digital signals are in the form of nanoscale surface plasmon polaritons [10]. Increase in Raman dispersion is an example of plasmonic waveguides [11].

The unique properties of the plasmonic waveguide, such as the high field intensity at the interface between the insulator and the metal, the resonance behavior, the ability to enclose the light in the nanoscale [6] and the low group speed has led to many applications. Examples of these applications are Conductivity and waveguide of light, Integrated Optical Circuits, Biological detection at single molecular level, light transmission of smaller apertures than light wavelengths and solar cells, Plasmonic waveguides can also be used for optical filtering applications in terahertz frequencies [12]. In the next section, we investigate supercontinuum in a plasmonic waveguide.

2. Equations

The supercontinuum generation process can be studied by solving the generalized NLS equation. As it is important to include the dispersive effects and intrapulse Raman scattering as accurately as possible. The single layer plasmonic waveguide is one of the simplest waveguides made on the smooth interface of a metal and a dielectric [9,13].

In this paper, we consider the silica as a nonlinear dielectric medium, silver as a metal medium. Equations governing the nonlinear pulse propagation in plasmonic waveguides [9] is obtained by using the first order perturbation and applying appropriate boundary conditions, then the simulation of supercontinuum pulse propagation in this waveguide is done. Figure 1 shows a schematic diagram of a single layer plasmonic waveguide, we consider the structure of a waveguide in the form of silica/silver consisting of a nonlinear dielectric layer of silica with a dielectric coefficient ϵ_2 and a sheet of silver metal with a dielectric coefficient ϵ_1 .

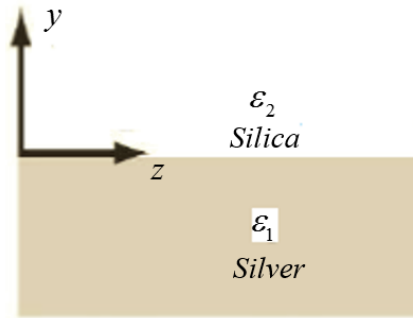


Fig. 1. A single layer plasmonic waveguide structure made of silica/silver.

The equations governing pulse propagation in a single layer plasmonic waveguide are as follows [9]:

$$i \frac{\partial u_1}{\partial \xi} - \frac{\text{sgn}(\beta_2)}{2} \frac{\partial^2 u_1}{\partial \tau^2} - \frac{i}{6} M \frac{\partial^3 u_1}{\partial \tau^3} + \frac{1}{24} M \frac{\partial^4 u_1}{\partial \tau^4} = M_{11}(u_1 |u_2|^2) - N_{11} u_1 \frac{\partial}{\partial \tau} |u_2|^2 \dots \quad (1)$$

$$-M_{12}(u_1 |u_3|^2) + N_{12} u_1 \frac{\partial}{\partial \tau} |u_3|^2 + i M_{11}^{(1)} \frac{\partial}{\partial \tau} (u_1 |u_2|^2) - i M_{12}^{(1)} \frac{\partial}{\partial \tau} (u_1 |u_3|^2)$$

$$i \frac{\partial u_2}{\partial \xi} - \frac{\text{sgn}(\beta_2)}{2} \frac{\partial^2 u_2}{\partial \tau^2} - \frac{i}{6} M \frac{\partial^3 u_2}{\partial \tau^3} + \frac{1}{24} M \frac{\partial^4 u_2}{\partial \tau^4} = U_{21}(u_2 |u_2|^2) - V_{21} u_2 \frac{\partial}{\partial \tau} |u_2|^2 \dots \quad (2)$$

$$-U_{22}(u_2 |u_3|^2) + V_{22} u_2 \frac{\partial}{\partial \tau} |u_3|^2 + i U_{21}^{(1)} \frac{\partial}{\partial \tau} (u_2 |u_2|^2) - i U_{22}^{(1)} \frac{\partial}{\partial \tau} (u_2 |u_3|^2)$$

$$i \frac{\partial u_3}{\partial \xi} - \frac{\text{sgn}(\beta_2)}{2} \frac{\partial^2 u_3}{\partial \tau^2} - \frac{i}{6} M \frac{\partial^3 u_3}{\partial \tau^3} + \frac{1}{24} M \frac{\partial^4 u_3}{\partial \tau^4} = K_{31}(u_3 |u_2|^2) - L_{31} u_3 \frac{\partial}{\partial \tau} |u_2|^2 \dots \quad (3)$$

$$-K_{32}(u_3 |u_3|^2) + L_{32} u_3 \frac{\partial}{\partial \tau} |u_3|^2 + i K_{31}^{(1)} \frac{\partial}{\partial \tau} (u_3 |u_2|^2) - i K_{32}^{(1)} \frac{\partial}{\partial \tau} (u_3 |u_3|^2)$$

Which the parameters used in the three above relationships are defined as:

$$\begin{aligned}
 M &= \frac{\beta_3 L_D}{T_0^3}, M' = \frac{\beta_4 L_D}{T_0^4}, L_D = \frac{T_0}{|\beta_2|}, M_{11} = \gamma_{11} L_D, N_{11} = \gamma_{11} L_D \frac{T_R}{T_0}, M_{12} = \gamma_{12} L_D \\
 N_{12} &= \gamma_{12} L_D \frac{T_R}{T_0}, M_{11}^{(1)} = \gamma_{11}^{(1)} \frac{L_D}{T_0}, M_{12}^{(1)} = \gamma_{12}^{(1)} \frac{L_D}{T_0}, U_{21} = \gamma_{21} L_D, V_{21} = \gamma_{21} L_D \frac{T_R}{T_0}, U_{22} = \gamma_{22} L_D \\
 V_{22} &= \gamma_{22} L_D \frac{T_R}{T_0}, U_{21}^{(1)} = \gamma_{21}^{(1)} \frac{L_D}{T_0}, U_{22}^{(1)} = \gamma_{22}^{(1)} \frac{L_D}{T_0}, K_{31} = \gamma_{31} L_D, L_{31} = \gamma_{31} L_D \frac{T_R}{T_0}, K_{32} = \gamma_{32} L_D \\
 L_{32} &= \gamma_{32} L_D \frac{T_R}{T_0}, K_{31}^{(1)} = \gamma_{31}^{(1)} \frac{L_D}{T_0}, K_{32}^{(1)} = \gamma_{32}^{(1)} \frac{L_D}{T_0}
 \end{aligned} \tag{4}$$

L_D and T_0 are the dispersion length and the input peak width, respectively. The first moment of Raman's response function (T_R) is also defined as follows:

$$T_R \equiv \int_0^\infty tR(t)dt \approx f_R \int_0^\infty th_R(t)dt = f_R \left. \frac{d(\text{Im} \tilde{h}_R)}{d(\Delta\omega)} \right|_{\Delta\omega=0} \tag{5}$$

The nonlinear parameters γ in the above equations are calculated as:

$$\gamma_1 = P_0 \frac{n(\omega)n_2(\omega)\omega}{2C^2\beta^2\varepsilon_0\varepsilon_2^2k_2} \cdot \frac{1}{\left(\frac{1}{2\varepsilon_1k_1} + \frac{1}{2\varepsilon_2k_2}\right)} \cdot \frac{1}{\left(\frac{1}{2k_1} + \frac{1}{2k_2}\right)} \tag{6}$$

$$\gamma_{11} = k_2^2\gamma_1, \gamma_{12} = \beta^2\gamma_1, \gamma_{11}^{(1)} = \frac{\partial\gamma_{11}}{\partial\omega}, \gamma_{12}^{(1)} = \frac{\partial\gamma_{12}}{\partial\omega}$$

$$\gamma_2 = P_0 \frac{2n(\omega)n_2(\omega)\omega k_2}{C^2\beta^2\varepsilon_0\varepsilon_2^4} \cdot \frac{1}{\left(\frac{k_1}{2\varepsilon_1^2} + \frac{k_2}{2\varepsilon_2^2}\right)} \cdot \frac{1}{\left(\frac{1}{2\varepsilon_1k_1} + \frac{1}{2\varepsilon_2k_2}\right)} \tag{7}$$

$$\gamma_{21} = k_2^2\gamma_2, \gamma_{22} = \beta^2\gamma_2, \gamma_{21}^{(1)} = \frac{\partial\gamma_{21}}{\partial\omega}, \gamma_{22}^{(1)} = \frac{\partial\gamma_{22}}{\partial\omega}$$

$$\gamma_3 = P_0 \frac{n(\omega)n_2(\omega)\omega}{2C^2\beta^2\varepsilon_0\varepsilon_2^4k_2} \cdot \frac{1}{\left(\frac{1}{2k_1\varepsilon_1^2} + \frac{1}{2k_2\varepsilon_2^2}\right)} \cdot \frac{1}{\left(\frac{1}{2\varepsilon_1k_1} + \frac{1}{2\varepsilon_2k_2}\right)} \quad (8)$$

$$\gamma_{31} = k_2^2\gamma_3, \gamma_{32} = \beta^2\gamma_3, \gamma_{31}^{(1)} = \frac{\partial\gamma_{31}}{\partial\omega}, \gamma_{32}^{(1)} = \frac{\partial\gamma_{32}}{\partial\omega}$$

C is the speed of light in a vacuum and P_0 is the input peak power, β is the propagation constant regardless of nonlinear effects and is written as follows [9]:

$$\beta = k_0 \sqrt{\frac{\varepsilon_1\varepsilon_2}{\varepsilon_1 + \varepsilon_2}} \quad (9)$$

In this step we ignore the imaginary part of dielectric constant of silver ε_1 but the effect of the imaginary part is used for calculating the propagation length to show the ignorance is acceptable or not [14]:

$$\varepsilon_1 = 1 - \frac{\omega_p^2}{\omega^2} \quad (10)$$

ω_p is plasma frequency and ε_2 is silica dielectric coefficient, $n(\omega)$ is calculated from the Sellmeier relationship[15]:

$$n^2(\omega) = 1 + \sum_{j=1}^m \frac{B_j\omega_j^2}{\omega_j^2 - \omega^2} \quad (11)$$

Where ω_j is the resonant frequency and B_j is the j^{th} resonant power, k_1 and k_2 in the above equations are the wave vector components in the x direction and are written as follows:

$$\begin{aligned} k_1^2 &= \beta^2 - k_0^2\varepsilon_1 \\ k_2^2 &= \beta^2 - k_0^2\varepsilon_2 \end{aligned} \quad (12)$$

Equations 1 to 3 are coupled equations for propagation in a nonlinear plasmonic waveguide with nonlinear Kerr effect, the above parameters determine the pulse propagation behavior, namely the dispersion and nonlinear effects that are studied numerically in the next section.

3. Simulation of Dispersion, Propagation Length and Nonlinear Length

In this section, the propagation of different orders of fundamental soliton are considered:

$$u = N \operatorname{sech}(\tau) \quad (13)$$

And launching to waveguide for simulating Equations (6) to (8) also the effects of nonlinear and dispersive effects on are studied, N represents the order of solitons and is obtained from the following equation:

$$N^2 = \frac{L_D}{L_{NL}} = \frac{\gamma P_0 T_0}{|\beta_2|} \quad (14)$$

Where γ and β_2 are the dispersion and nonlinearity length respectively.

Dispersion is one of the important parameters for supercontinuum study, various orders of dispersion are obtained from derivatives of the propagation constant respect to frequency which is calculated from equation (9) for the plasmonic waveguide. The dielectric constant of silver ϵ_1 and for silica is ϵ_2 which is obtained according to the Sellmeier relation.

Due to the complexity of the relationships, the dispersion is calculated using numerical methods and is plotted in Figure (2) in terms of frequency and wavelength. For SC generation GVD must be near zero dispersion as shown in Figure(2) the second order zero dispersion is at $x=0.06256$, which is equivalent to the wavelength of $\lambda = 2.215\mu\text{m}$. Therefore, to create a supercontinuum, a wavelength close to zero ($\lambda = 2.22\mu\text{m}$ ($x = 0.0622$)) with negative dispersion is selected.

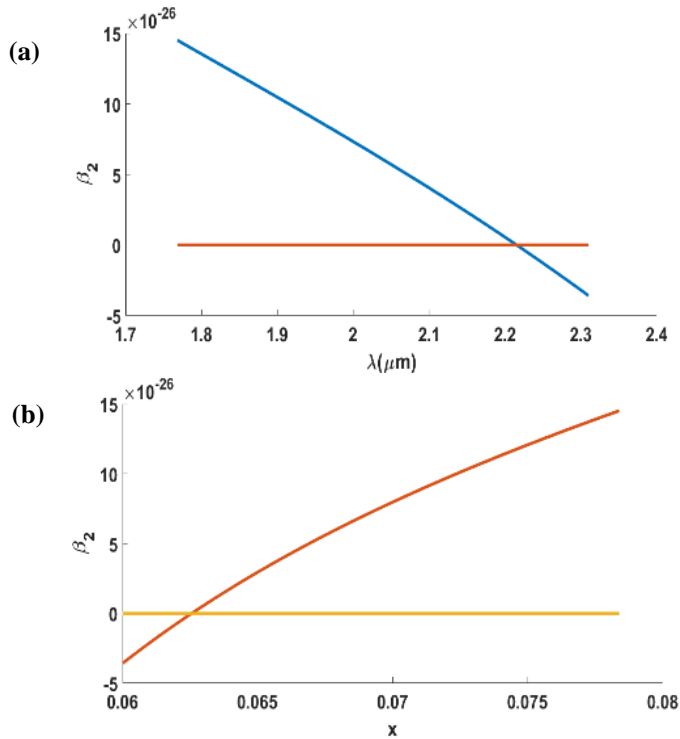


Fig. 2. Dispersion (s^2/m) in a plasmonic waveguide in terms of (a) wavelength, (b) x (dimensionless frequency).

Another parameter that is very important is the propagation length that must be calculated in a plasmonic waveguide, the emission length is equal to the reverse half of the imaginary part of the propagation constant when the dielectric constant of the metal is expressed in a complex way. Figure(3) shows the propagation length in dimensionless frequency and wavelength for a plasmonic waveguide composed of silver and silica, as shown in the figure, the propagation length decreases with increasing frequency, which we also expected.

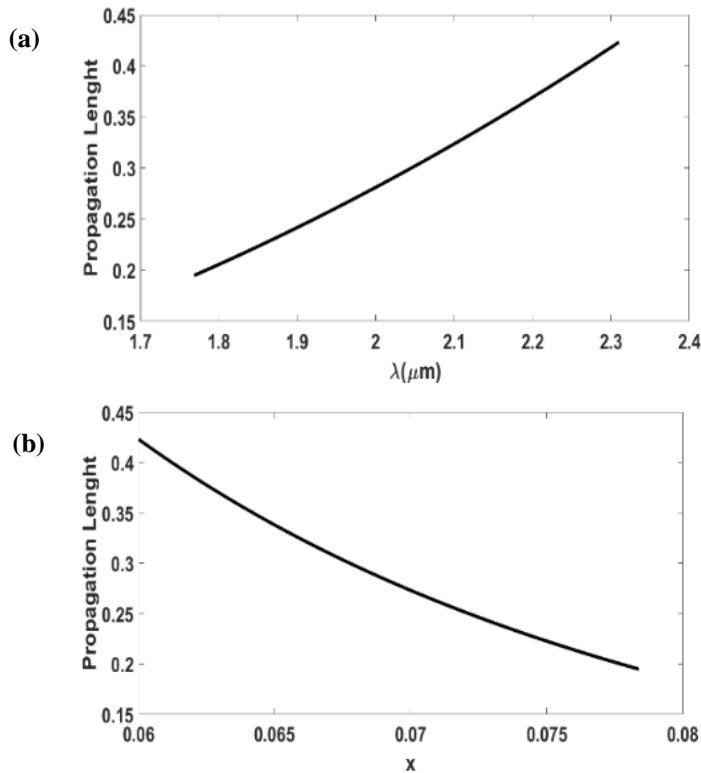


Fig. 3. Propagation length (m) in plasmonic waveguide in terms of (a) wavelength, (b) x (dimensionless frequency)

Another important parameter for creating a supercontinuum is nonlinear length, according to the three nonlinear equations governing the nonlinear plasmonic waveguide (Equations (1), (2) and (3)), three nonlinear lengths in Figure (4) are plotted in terms of x , as can be seen, as the frequency increases, the nonlinear length initially decreases as expected, but, due to decreasing the sub wavelength confinement of the wave with increasing frequency the nonlinear effect increase and the nonlinear length decrease.

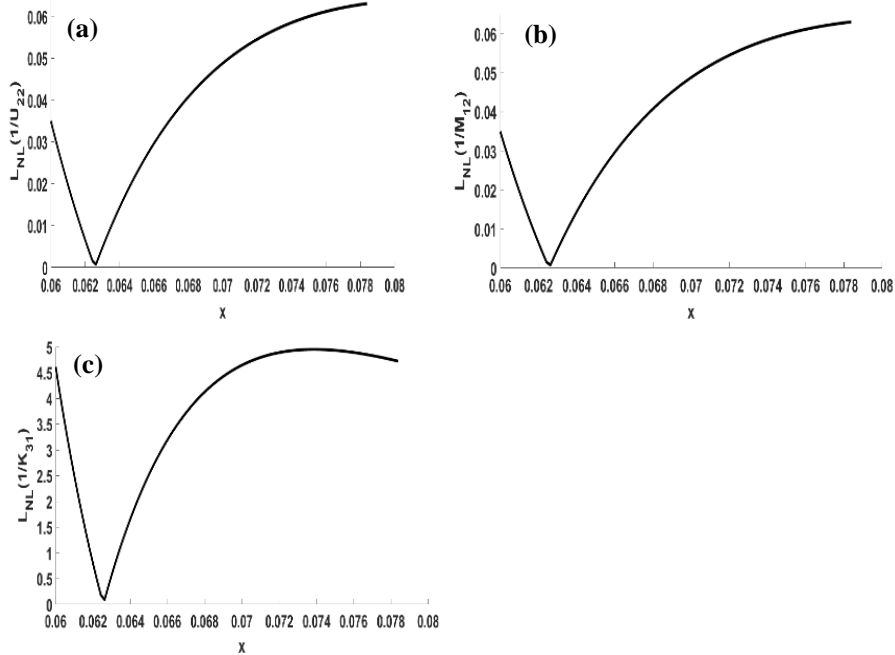


Fig. 4. Nonlinear length (m) changes in plasmonic waveguide in terms of x (dimensionless frequency): (a) $1/K_{31}$, (b) $1/U_{22}$, (c) $1/M_{12}$

Fortunately, according to the figure (4), at $x = 0.0622$ nonlinear length is small and is the order of propagation length at this selected dimensionless frequency. By decreasing nonlinear length, the nonlinear effects are increased which is suitable for continuum generation.

4. Simulation of 10th, 15th and 30th Order Soliton Propagation

In this section, soliton propagation of 10th, 15th and 30th order are simulated by using Equations (1) to (3), as mentioned dispersion, chooses to close to zero, according to Figure (3), appropriate point where the dispersion is close to zero, selected to the value of $x = 0.0622$ is considered and as a result the desired parameters for simulation are obtained as a table (1).

Table 1. Selected and calculated parameters for simulation.

$X(y)$ -(dimensionless)	0.0622
β_2	$-0.44 \times 10^{-26} \frac{s^2}{m}$
L_{NL}	$3.8 \times 10^{-3} m$
L (Propagation Length)	0.38 m
T_0	$400 \times 10^{-15} s$

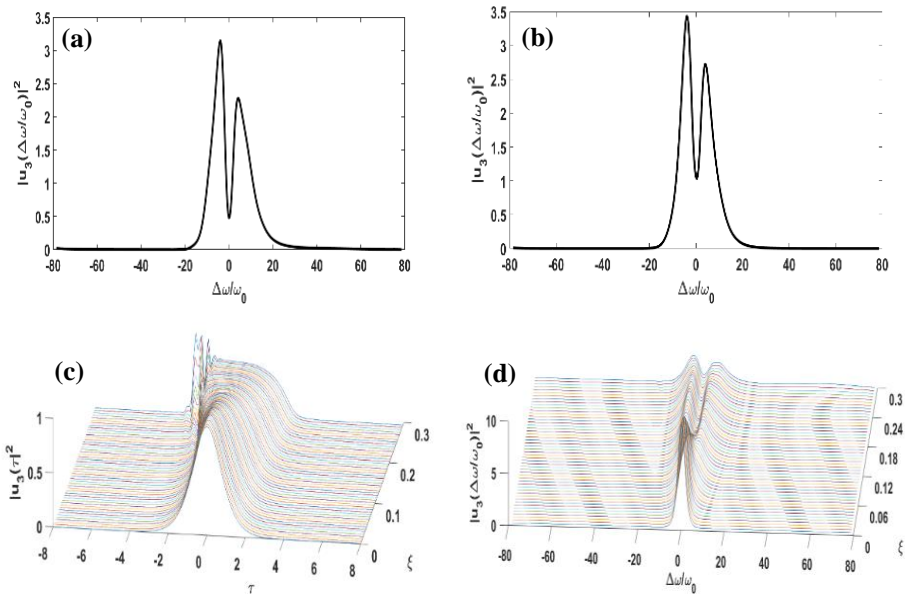


Fig. 5. Pulse propagation in the domain of time and frequency along the waveguide with $N = 10$ and considering the nonlinear effects of modulation, Raman scattering, self-steepening and 2nd, 3rd and 4th order dispersion (a) Pulse spectrum in $\xi = 0.18$ (b) Pulse spectrum in $\xi = 0.24$ (c) Pulse propagation along wavelength in the time domain (d) Pulse spectrum propagation along the waveguide.

As shown in Figure (5), the pulse is launched to the plasmonic waveguide, as it propagates gradually deforms in time domain Figure (5c) and naturally in frequency domain Figure (5d) under the influence of nonlinear and dispersion effects.

In Figure (5d), the evolution of the pulse spectrum along the waveguide is simulated, as shown in the figure, after the propagation of the pulse in the frequency domain, it is divided into two peaks and the central frequency of the pulse is converted into two frequencies less and more than frequency center, which is called frequency conversion but our goal of producing a supercontinuum is not being achieved.

For greater clarity in Figures (5a and 5b), the pulse spectrum is plotted at lengths of 0.18 and 0.24. As can be clearly seen, the frequency conversion has taken place, but the supercontinuum has not been produced. To produce the supercontinuum, increase the normalization length to have more nonlinear and dispersion effects and achieve the desired results.

In Figure (6), simulations are performed for further normalization length and pulse propagation in the time domain and soliton frequency of order 10 is shown. As shown in Figure (6e), as the length increases, the frequency spectrum increases and is braked into more pulses.

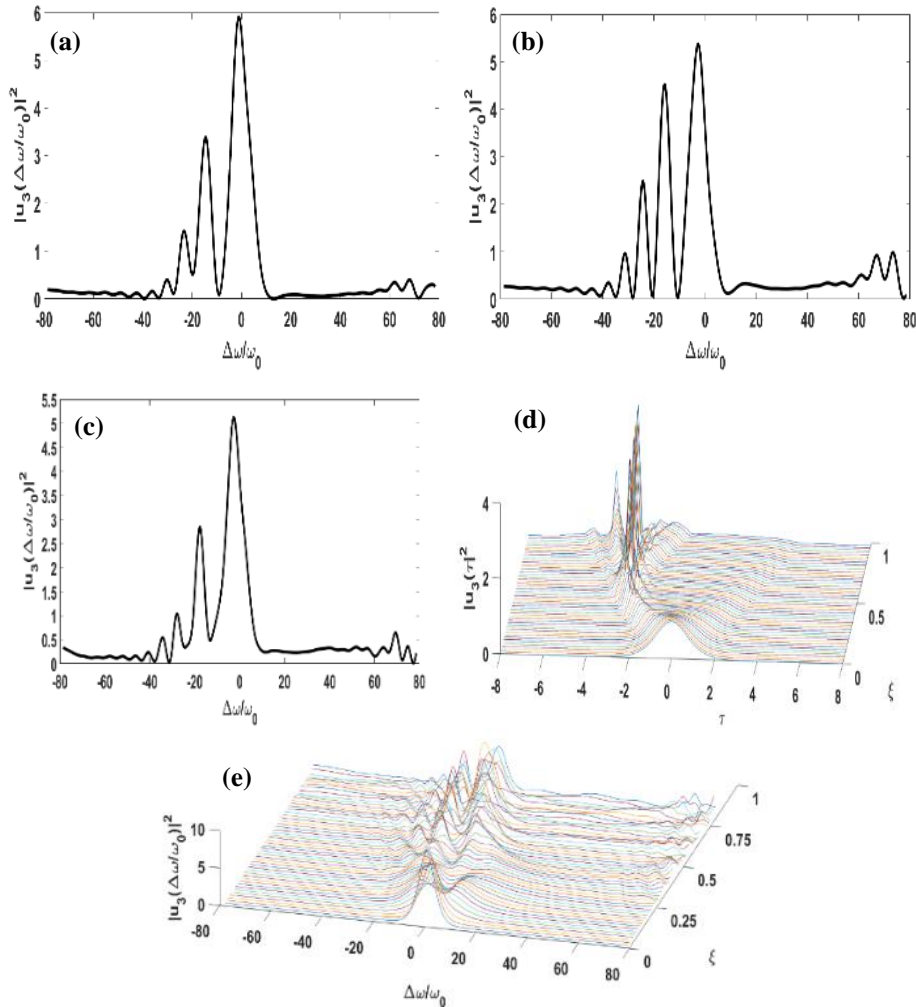


Fig. 6. Pulse propagation in the domain of time and frequency along the waveguide with $N = 10$ and considering the nonlinear effects of modulation, Raman scattering, self-steepening and 2nd, 3rd and 4th order dispersion (a) Pulse spectrum in $\xi = 0.66$ (b) Pulse spectrum in $\xi = 0.68$ (c) Pulse spectrum in $\xi = 0.8$ (d) Pulse propagation along wavelength in the time domain (e) Pulse spectrum propagation along the waveguide

Three examples of spectra at different lengths are shown in Figures (6a to c), as can be seen in each, more than 2 spectral peaks have occurred and the

spectrum has extended but this extension is not seen everywhere and does not seem to be acceptable for continuum production, Therefore, it seems that increasing ξ at this stage cannot solve the problem. In the next step, the simulation is performed for a higher soliton order. In Figure (7), while maintaining the previous parameters, the soliton order is increased to 15 at $\xi = 0.24$ and $\xi = 0.27$.

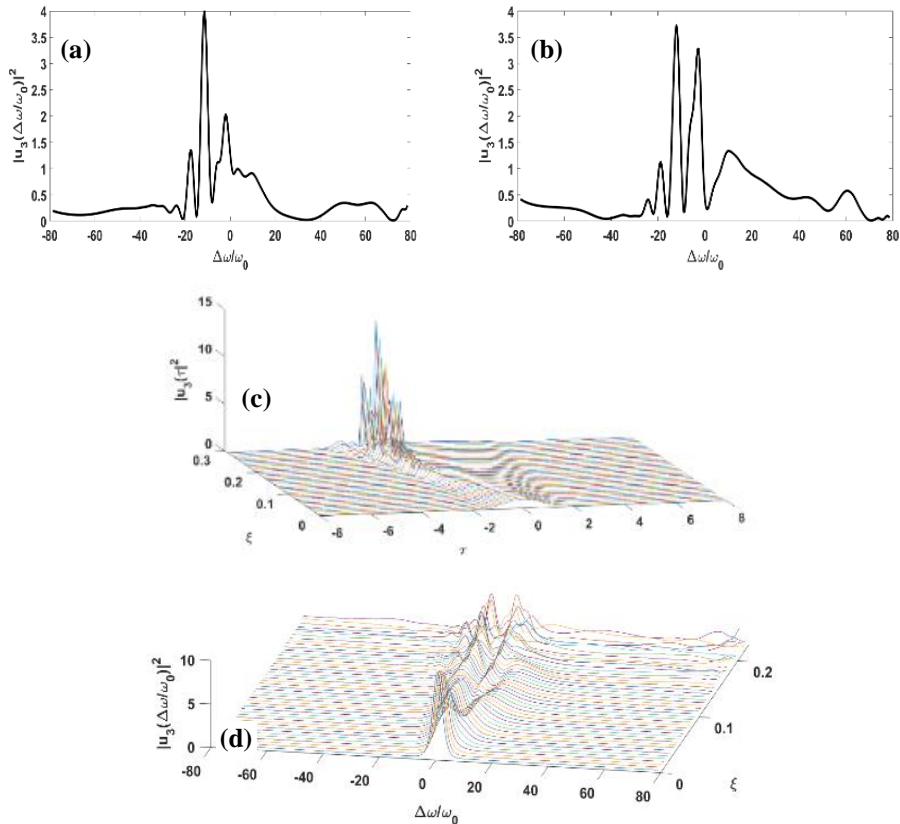
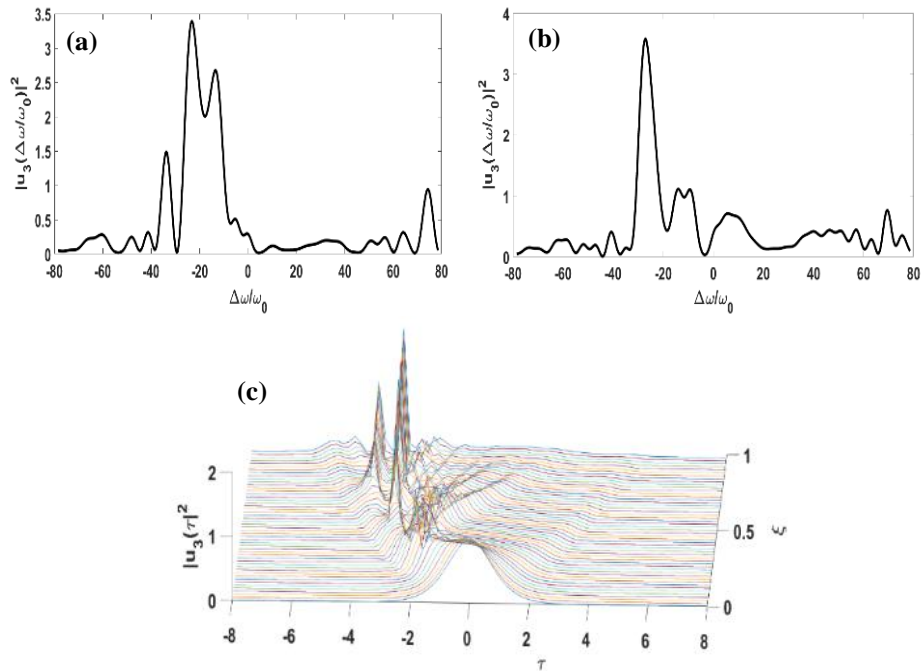


Fig. 7. Pulse propagation in the domain of time and frequency along the waveguide with $N = 15$ and considering the nonlinear effects of modulation, Raman scattering, self-steepening and 2nd, 3rd and 4th order dispersion (a) Pulse spectrum in $\xi = 0.24$ (b) Pulse spectrum in $\xi = 0.27$ (c) Pulse propagation along wavelength in the time domain (d) Pulse spectrum propagation along the waveguide.

As can be seen in Figure (7), the frequency spectrum increases with increasing soliton order and is divided into more pulses. In Figures (7a and 7b) the spectrum is shown in different lengths, at this stage, too, extension is not seen everywhere, and SC is not produced, therefore, it seems that increasing the soliton level to 15 at this stage still does not solve the problem. Next, the simulation is performed for 15th order soliton with longer normalization length, in Figure (8a and 8b), the spectrum is shown at different lengths for 15th order soliton at $\xi = 0.52$ and $\xi = 0.7$.



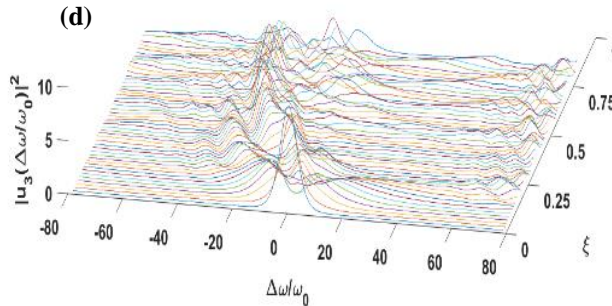


Fig. 8. Pulse propagation in time and frequency domain along the waveguide with $N = 15$ by considering the nonlinear effects of modulation, Raman scattering, self-steepening and 2nd, 3rd and 4th order dispersion (a) Pulse spectrum in $\xi = 0.52$ (b) Pulse spectrum in $\xi = 0.7$ (c) Pulse propagation along wavelength in the time domain (d) Pulse spectrum propagation along the waveguide.

Figures (8c and 8d) shows that the 15th order soliton tries to extend the spectrum, but the expected result is still not observed however, there are more peaks than in Figure 7. Figure (9) shows the pulse propagation in the time and frequency domain for a 30th order soliton with all dispersion and nonlinear effects along the fiber.

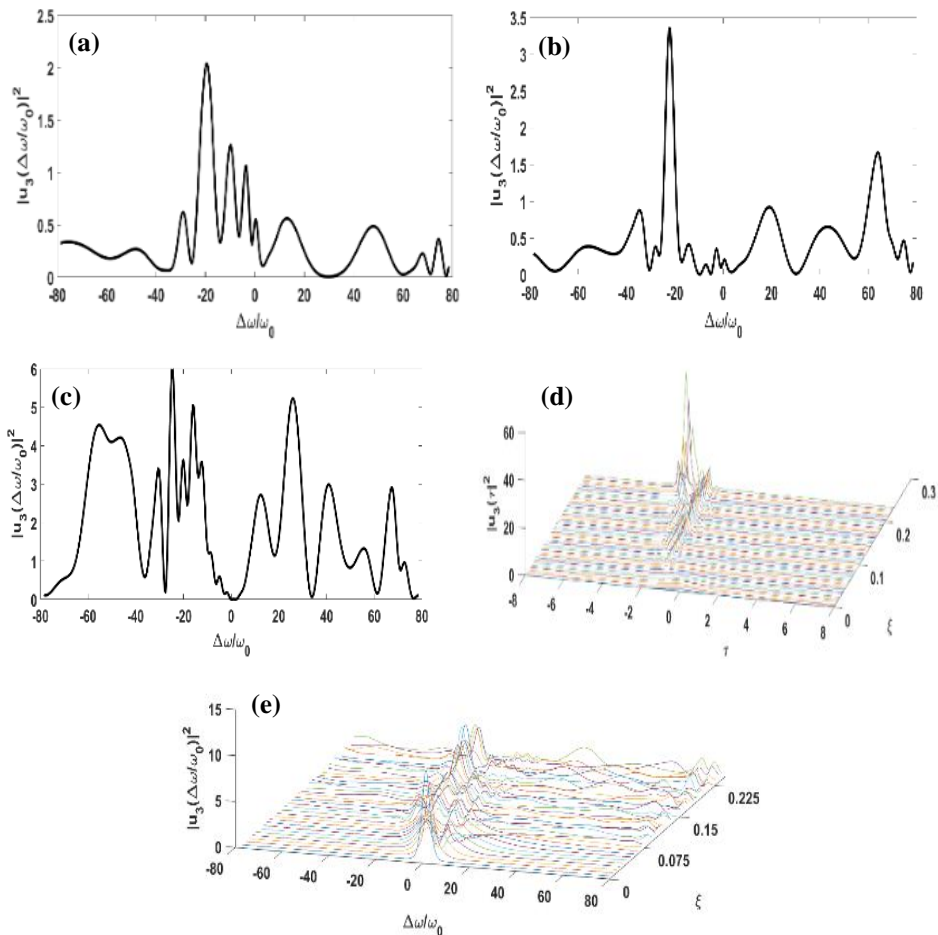


Fig. 9. Pulse propagation in the domain of time and frequency along the waveguide with $N = 30$ and considering the nonlinear effects of modulation, Raman scattering, self-steepening and 2nd, 3rd and 4th order dispersion (a) Pulse spectrum in $\xi = 0.12$ (b) Pulse spectrum in $\xi = 0.16$ (c) Pulse spectrum in $\xi = 0.23$ (d) Pulse propagation along wavelength in the time domain (e) Pulse spectrum propagation along the waveguide

In Figure (9d) propagation of pulse in the time domain is simulated. At the beginning of the waveguide, 30th order soliton is launched and during the propagation under the influence of nonlinear effects and dispersion is deformed and broken into side pulses. In Figure (9e) the propagation of the same 30th order soliton in the frequency domain is simulated.

The pulse spectrum changes under the influence of various nonlinear and dispersion effects during propagation, and new frequency components are added or shifted. If we want to have a detailed study of the pulse spectrum, we must look at it in any point along the waveguide. According to our goal, which was to produce supercontinuum, we tried to select the points where the most frequency transformations occurred.

For example, in Figures (9a to c), the pulse spectrum is plotted in three normalized lengths of 0.12, 0.16 and 0.23 in two dimensions then we have tried to select the best extended spectrum in these lengths, comparing their shapes, it can be seen that the number of distributed frequency peaks during length of 0.23 was the best which we have expected, with increasing soliton order, the amplitude of NSRs grows relatively faster.

NSRs are non-solitonic radiations emitted by third and higher-order dispersions and emitted in the form of dispersive waves (DWs), Interestingly, this rapid growth is observed at the shortest normalized length i.e., 0.12, this indicates a supercontinuum generation according to the results.

5. Investigation of Different States of the Effects of Dispersion and Nonlinear Coefficients in the Production of Supercontinuum for 30th Order Soliton

In this section, different states of dispersions and nonlinearities for $T_0 = 400\text{e-}15$ and 30th order soliton are investigated. Figure (10) shows a state in which only the third-order dispersion is considered for the 30th order soliton. Theoretically, the presence of a 30th order dispersion (3OD) is a prerequisite to produce DWs when the optical pulse is propagated as a soliton, it should be noted that a minimum value of β_3 is required before starting of NSR, which strongly depends on the order of soliton (N). For higher order soliton, lower β_3 value is needed.

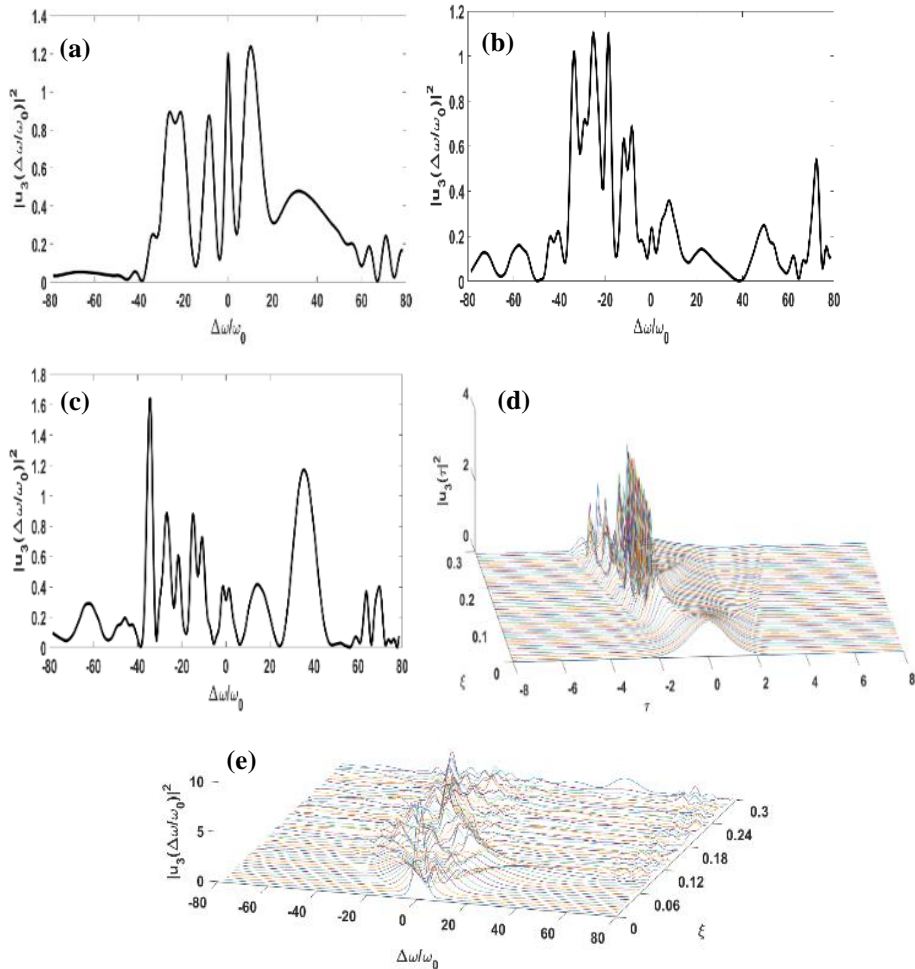


Fig. 10. Pulse propagation in the time and frequency domain along the waveguide with $N = 30$ and only in the presence of third-order dispersion effect (a) Pulse spectrum in $\xi = 0.09$ (b) Pulse spectrum in $\xi = 0.26$ (c) Pulse spectrum in $\xi = 0.30$ (d) Pulse propagation along wavelength in the time domain (e) Pulse spectrum propagation along the waveguide.

As mentioned earlier and shown in Figure (10), the third order dispersion (3OD) has an important effect on the spectral broadening. As it seen in the beginning of propagation of pulse spectrum in figure (10e) a good spectral broadening is observed at the minimum normalized length $\xi = 0.09$. The broadening of pulse is shifted to the right because 3OD is negative. If the 3OD

coefficient is negative, spectral broadening occurs at the low frequency side and vice versa.

The second case considered in Figure (11) is just the effect of 4th order dispersion β_4 , after 3OD is a significant term in the equations cause to produce dual NSR radiation. The current theory shows that a positive 4OD always produces a conjugate radiation such that a blue and red peak is observed in the output spectrum.

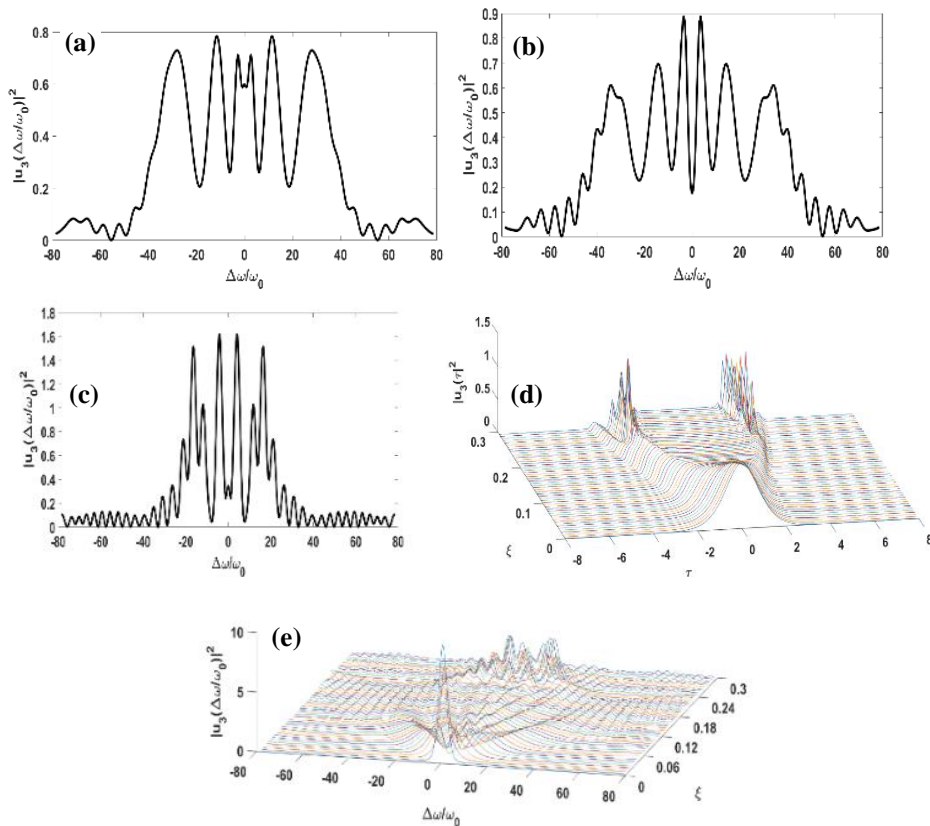


Fig. 11. Pulse propagation in the domain of time and frequency along the waveguide with $N = 30$ and only in the presence of fourth-order dispersion effect (a) Pulse spectrum in $\xi = 0.10$ (b) Pulse spectrum in $\xi = 0.12$ (c) Pulse spectrum in $\xi = 0.25$ (d) Pulse propagation along wavelength in the time domain (e) Pulse spectrum propagation along the waveguide.

Numerical simulation confirms that in the absence of a higher order nonlinear effect and dispersion terms, dual peaks generated by the 4OD are symmetrically located in the frequency domain. In this case, more spectral broadening is observed symmetrically.

From the simulations all positive even-order dispersion terms (i.e., 8OD, 6OD, 4OD, etc.) propagate conjugate radiation, and all positive odd-order dispersion terms (i.e., 7OD, 5OD, 3OD, etc.) can produce blue radiation and when the sign of odd dispersion coefficient is inverted, the radiation is on the red side.

Figure (12) shows only the effect of Raman scattering (IPRS) on the output pulse spectrum in the presence of 4OD. Due to the Raman scattering effect, a continuous transfer of energy from higher frequencies to lower frequencies is expected to cause an asymmetric spectrum, but because DWs are generated exactly after the soliton fission process, their amplitudes and frequencies are not initially greatly affected by the subsequent energy transfer due to IPRS.

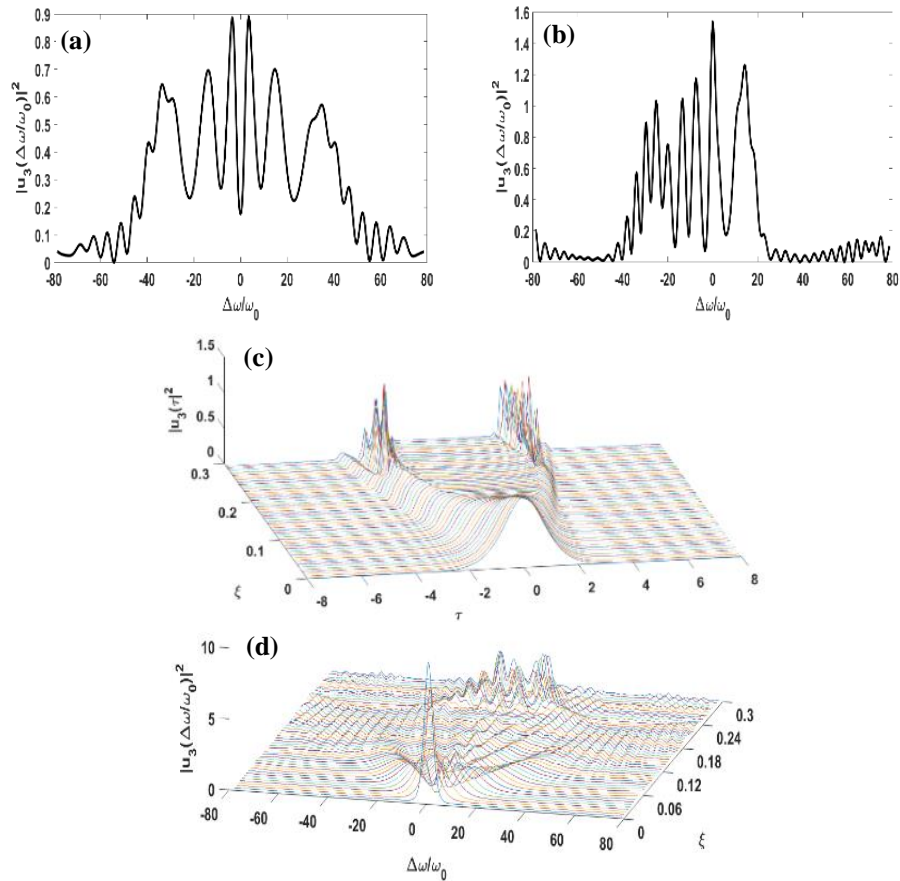


Fig. 12. Pulse propagation in the domain of time and frequency along the waveguide with $N = 30$ and only in the presence of fourth-order dispersion effect and nonlinear Raman scattering (a) Pulse spectrum in $\xi = 0.12$ (b) Pulse spectrum in $\xi = 0.25$ (c) Pulse propagation along wavelength in the time domain (d) Pulse spectrum propagation along the waveguide.

As shown in Figure (12), the spectrum initially tries to maintain symmetry, but then, as it progresses along the waveguide, the extension of the spectrum gradually loses its symmetry and, due to the energy transfer caused by IPRS, the negative frequency direction extends.

Figure (13) shows the pulse propagation along the plasmonic waveguide in a state that includes the effects of 3OD, 4OD and IPRS simultaneously, in this case an output spectrum is obtained under a more general and realistic state, the spectrum changes dramatically compared to the previous shape.

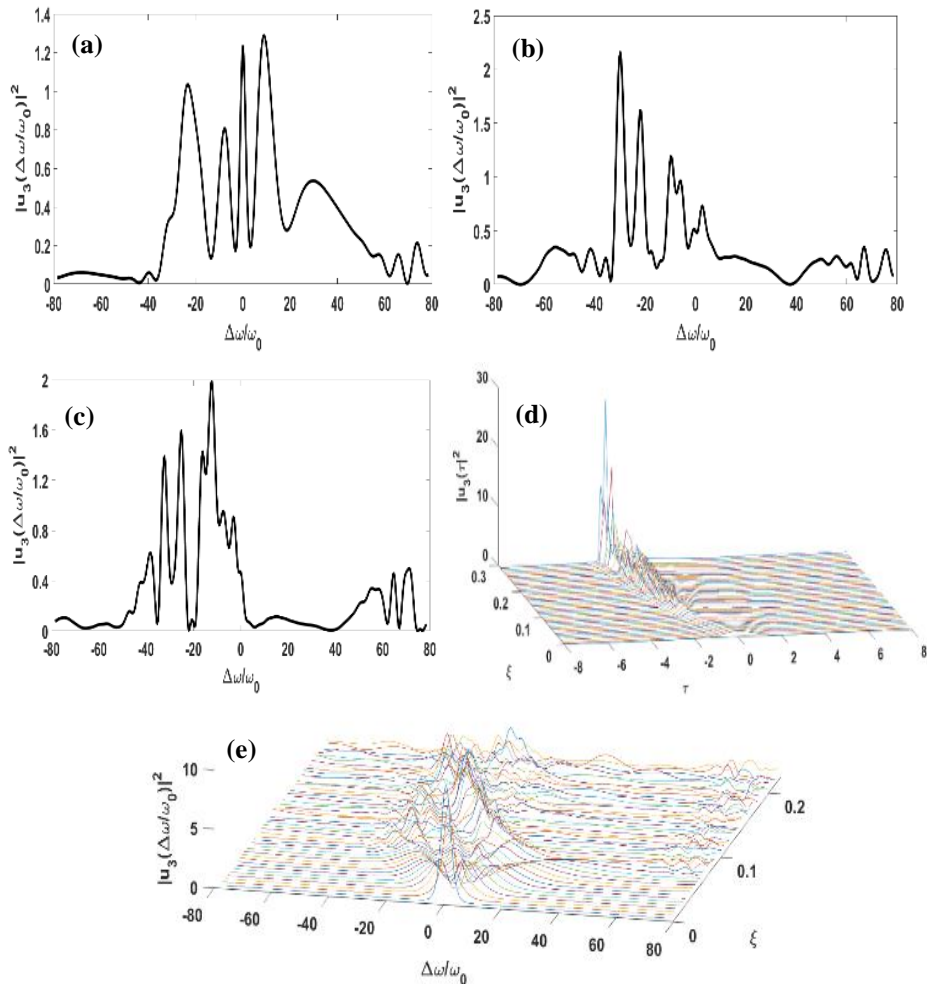
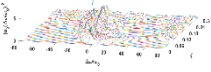
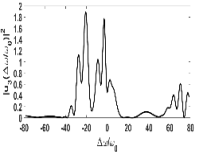
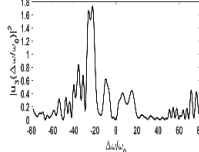
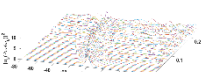
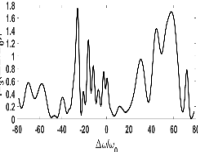
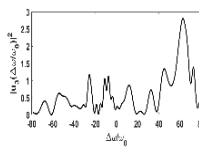
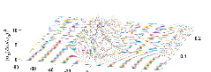
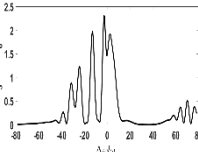
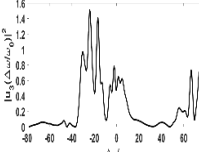
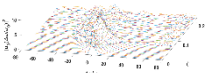
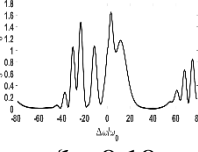
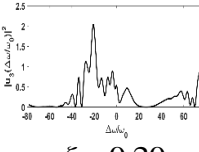

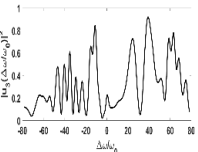
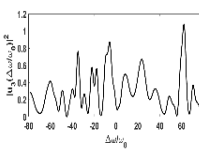


Fig. 13. Pulse propagation in the domain of time and frequency along the waveguide with $N = 30$ including the effects of 3OD, 4OD and IPRS (a) Pulse spectrum in $\xi = 0.08$ (b) Pulse spectrum in $\xi = 0.22$ (c) Pulse spectrum in $\xi = 0.25$ (d) Pulse propagation along wavelength in the time domain (e) Pulse spectrum propagation along the waveguide.

Table. 2. Propagation of pulse spectrum along plasmonic waveguide with $N = 30$

High-order effects in different modes	Pulse spectral propagation during propagation	Pulse spectrum at a point of propagation length		Maximum of $\frac{\Delta\omega}{\omega_0}$
Fourth order dispersion and self-steepening (4OD, SS)		 $\xi = 0.12$	 $\xi = 0.28$	160
Third order dispersion and self-steepening (3OD, SS)		 $\xi = 0.22$	 $\xi = 0.24$	160
Third & fourth order dispersion (3OD, 4OD)		 $\xi = 0.12$	 $\xi = 0.24$	120
Third order dispersion & Raman scattering (3OD, IPRS)		 $\xi = 0.10$	 $\xi = 0.20$	140
All effects with increasing normalized length		 $\xi = 0.42$	 $\xi = 0.48$	160

As shown in Figure (12), only with the IPRS effect, the spectrum initially tries to maintain its symmetry because the Raman scattering effect does not initially have much effect on the amplitude and frequencies of the DW but, by inserting the 3OD effect in Figure (13), the change in the output spectrum, as expected, is clearly visible from the beginning towards the negative frequencies, and in less than 0.10 the amplitude of the spectrum towards the negative frequencies is very good. In Figure (12) the amplitude of the spectrum and the production of peaks are significant, although in Figure (13) it is easier to separate the spectrum to obtain a specific frequency and the intensity of the peaks is higher.

In particular, it can be seen that the red (blue) side of the pulse spectrum contains more (less) pulse energy than the blue (red) side, because when $\beta_3 \neq 0$ ($\beta_3 = 0$), 3OD creates an NSR peak on the red (blue) side of the spectrum, In the following, other states of pulse spectrum propagation along the plasmonic waveguide with $N = 30$ are summarized in Table (2).

Figures (10) to (13) as well as Table (2) for 30th order soliton show different dispersion and nonlinear states, which in addition to 10th and 15th order soliton states, a good spectral range is observed, compared to the 30th order soliton state of figure (9), (all effect together) also shows a better spectral broadening, Because in the previous case, when all the effects were considered together, some effects neutralize the effect of the other factor in the spectral broadening. But here, by considering only two or three effects of dispersion and nonlinearities, these effects amplify each other and cause more spectral broadening and thus produce more frequency components, as it has reached the maximum peak at a constant width.

In Table (2), by considering the first and second row very good width is observed, we conclude that the nonlinear effect of self-steepening plays a key role in spectral broadening, also in the last row of the table for 30th order soliton, with the increase of normalized length and the presence of all nonlinear effects and dispersion, good spectral broadening and expected supercontinuum production is observed.

6. Conclusion

In this article, the formation of a supercontinuum in a nonlinear plasmonic waveguide consisting of silver and a nonlinear silica material was investigated and it was found that the negative or positive dispersion as well as the main

characteristics of the spectrum determine which type of nonlinear effects contribute to the formation of the supercontinuum.

The suitable point for producing supercontinuum near zero dispersion was selected, then with the obtained parameters, the propagation of light solitons of 10, 15 and 30 orders was simulated.

In the next step, the same work was done by maintaining the previous parameters for 15th order soliton, in which case the frequency spectrum the number of frequency peaks distributed during length 0.21 was the best, and as expected with increasing soliton order, the amplitude of NSRs grew relatively faster and more energy was generated, however, this rapid growth was observed at the lowest normalization length 0.12 and this was a good supercontinuum according to the results.

Since the third-order dispersion (3OD) is the initial condition to produce DWs, so the pulse propagation in the frequency domain along the wavelength with $N = 30$ was observed only in the presence of the third-order dispersion effect.

Pulse propagation simulations were performed along the plasmonic waveguide in a state that included the effects of 3OD, 4OD, and IPRS simultaneously, which showed an output spectrum under a more realistic state. Also, in Table (2) for 30th order soliton, various dispersion and nonlinear states were shown, in addition a good spectral broadening was observed in comparison with the 10th and 15th order soliton, it showed a better spectral broadening than the 30th order soliton, taking into account all the effects together.

Self-steepening plays a very significant role in the spectral broadening and production of supercontinuum in the plasmonic waveguide. Finally nonlinear plasmonic waveguides are suitable for integrated photonics because of subwavelength confinement of plasmonic waveguides.

References

- [1] A.V. Husakou, J. Herrmann. Supercontinuum generation of higher order solitons by fission in photonic crystal fibers. *Phys.Rev. Lett*, 87, (2001) 203901. Available: <https://doi.org/10.1103/PhysRevLett.87.203901>
- [2] J. Herrmann et al. *Experimental evidence for supercontinuum generation by fission of higher order soliton in photonic fibers*. *Phys. Rev. Lett*, 88, (2002) 173901. Available: <https://doi.org/10.1103/PhysRevLett.88.173901>
- [3] J. M. Dudley, G. Genty, S. Coen. *Supercontinuum generation in photonic crystal fiber*. *Rev. Mod. Phys.* 78, (2006) 1135–1184. Available: <https://doi.org/10.1103/RevModPhys.78.1135>
- [4] A. M. Zheltikov. *supercontinuum generation by ultrashort laser pulses*. *Phys–Uspekhi*. 49, (2006) 605–628. Available: <https://doi.org/10.3367/UFNr.0176.200606d.0623>
- [5] J. M. Dudley, J. R. Taylor. *Ten years of nonlinear optics in photonic crystal fiber*. *Nature Photonics*, 3, (2009) 85–90. Available: <https://doi.org/10.1038/nphoton.2008.285>
- [6] Q. Lu, C. Zou, D. Chen, P. Zhou, G. Wu. *Extreme light confinement and low loss in triangle hybrid plasmonic waveguide*. *Optics Communications*, Vol. 319, (2014) 141–146. Available: <https://doi.org/10.1016/j.optcom.2013.12.072>
- [7] Z. Muhammad, J. Alam, S. Aitchison, M. Mojahedi. *A marriage of convenience: Hybridization of surface plasmon and dielectric waveguide modes*. *Laser Photonics Rev.* 8, No. 3, (2014) 394–408. Available: <https://doi.org/10.1002/lpor.201300168>
- [8] H. A. Atwater. *The Promise of Plasmonics*, *Scientific American*. Vol. 296, No. 4, (2007) 56-63. Available: [doi:10.1038/scientificamerican0907-56sp](https://doi.org/10.1038/scientificamerican0907-56sp)
- [9] M. Dehghani, M. Hatami. *Raman scattering and self-steepening in nonlinear plasmonic waveguide pulse equation*, *Optical and Quantum Electronics* Springer, (2020) 52:124. Available: <https://doi.org/10.1007/s11082-020-2241-x>

- [10] D. Rukhlenko, P. Asanka, P. Malin. *Exact dispersion relation for nonlinear plasmonic waveguides*. Phys. Rev. B. (2011).
Available: <https://doi.org/10.1103/PhysRevB.84.113409>
- [11] B. Sharma, R. Frontiera, A. Henry, E. Ringe, R. P. van Duyne. *SERS: materials, applications, and the future*. 15, (2012) 16–25.
Available: [https://doi.org/10.1016/S1369-7021\(12\)70017-2](https://doi.org/10.1016/S1369-7021(12)70017-2)
- [12] H. Zhao, Y. Li, G. Zhang. *Study on the performance of bimetallic layer dielectric-loaded surface plasmon polariton waveguides*. Journal of optics, (2011) 115501. Available: <http://dx.doi.org/10.1088/2040-8978/13/11/115501>
- [13] R. Yang, M.A.G. Abushagur, Z. Lu. *Efficiently squeezing near infrared light into a 21 nm-by-24 nm nanospot*. Opt. Express 16, (2008) 20142–20148. Available: <https://doi.org/10.1364/OE.16.020142>
- [14] H. U. Yang, J. D'Archange, M. L. Sundheimer, E. Tucker, G. D. Boreman. *Optical dielectric function of silver*. Phys. Rev. 91, (2015) 1–11.
Available: <http://dx.doi.org/10.1103/PhysRevB.91.235137>
- [15] G.P. Agrawal. *Nonlinear Fiber Optics*. Sixth ed., Academic Press, USA. (2019). Available: <https://doi.org/10.1016/B978-0-12-817042-7.00008-7>